Topology Optimization of Regenerative Cooling Structure for Scramjet Combustion Chamber

T. Gao, X. Sun*, S. Chen, Z. Li, T. Song, T. Jing, Y. Liu and F. Qin
Corresponding author: sunxing@nwpu.edu.cn
Northwestern Polytechnical University, Xi'an, China.

Abstract: Regenerative cooling is an important thermal protection technology for hypersonic-engine combustors. Conventional straight cooling channels cannot readily adapt coolant distribution to non-uniform thermal loads, and they may suffer from insufficient local heat transfer and high wall-temperature risk. This study investigates the topology optimization design of regenerative cooling structures for a combustor. A density-based fluid-thermal coupling topology optimization model is developed on the OpenFOAM platform. The average temperature of the design domain is minimized, while constraints on the fluid volume fraction and power consumption are introduced to account for cooling performance and flow resistance. The optimization produces a regenerative cooling channel configuration with complex branching passages. A three-dimensional cooling structure is then constructed from the topology optimization result, and numerical simulations of flow and heat transfer are performed under different fluid volume fractions and inlet temperatures. Compared with a straight-channel configuration, the topology-optimized configuration reduces the channel-layer structural mass by 26% and significantly lowers the heated-surface temperature. Under the same fluid volume fraction, the average and maximum heated-surface temperatures of the topology-optimized configuration are reduced by 17.5% and 16.5%, respectively, at the low-temperature inlet condition; by 5.6% and 6.4% at the medium-temperature inlet condition; and by 3.3% and 4.4% at the high-temperature inlet condition. The results show that topology optimization can effectively improve wall-temperature control and coolant utilization efficiency in regenerative cooling structures, providing a reference for lightweight and efficient thermal protection design for hypersonic engines.

Keywords: Topology Optimization, Combustion Chamber, Regenerative Cooling, Heat Transfer.

1. Introduction

Airbreathing hypersonic engines, such as turbine-based combined-cycle (TBCC), rocket-based combined-cycle (RBCC), and dual-mode scramjet engines, are important propulsion concepts for wide-speed-range high-speed flight and reusable Earth-to-orbit transportation. As the flight Mach number and operating time increase, key components such as the combustor, isolator, nozzle, strut, and cavity are exposed to strong aerodynamic heating, combustion heat release, and non-uniform thermal loads. The thermal protection system must control wall temperature under strict mass and coolant-resource constraints [1–5]. Therefore, the design of efficient and lightweight thermal protection structures is a key issue in the engineering application of hypersonic engines.

Regenerative cooling uses engine fuel flowing through wall channels to absorb heat, thereby achieving structural cooling, fuel preheating, and energy recovery. For hydrocarbon fuels, high-temperature pyrolysis can further increase the heat sink [6–8]. However, regenerative cooling is strongly coupled with the combustor thermal environment. Wall heat flux, fuel-property variation, flow distribution, and cracking reactions jointly affect wall-temperature distribution and structural strength [8, 9]. As a result, empirical channel layouts and one-dimensional thermal-balance estimates alone are insufficient for the refined thermal protection design of combined-cycle engines under multi-mode and non-uniform thermal-load conditions.

Conventional regenerative cooling structures commonly use parallel straight channels or variable-area channels. These designs are simple, low-cost to manufacture, and suitable for engineering applications, and they have been widely used in thermal protection systems for liquid rocket engines and scramjet engines. In RBCC combustors, however, wall heat flux often exhibits pronounced axial and circumferential non-uniformity [10, 11]. Straight channels are prone to uneven flow distribution, insufficient local heat transfer, and overheating in high-heat-flux regions. Under supercritical pressure and thermal-cracking conditions, the thermophysical properties of hydrocarbon fuels vary sharply, which may further aggravate maldistribution, coking, and channel blockage [12, 13]. Therefore, cooling-channel design should evolve from empirical regular layouts toward optimization designs that account for thermal-load response, flow allocation, and structural constraints.

Topology optimization provides an effective tool for the free-form design of complex cooling channels. Borrvall and Petersson introduced a Brinkman penalization term into Stokes-flow problems, laying the foundation for fluid topology optimization [14]. Gersborg-Hansen et al. extended this approach to channel-flow and fluid-device design [15]. Density methods, adjoint methods, level-set methods, and moving morphable component methods have subsequently been used for flow and conjugate heat-transfer optimization. Othmer et al. promoted the implementation of continuous-adjoint topology optimization in OpenFOAM [16, 17], and Nilsson systematically described the OpenFOAM adjoint optimization solver [18]. Matsumori et al. and Kontoleontos et al. studied fluid-thermal coupling topology optimization, heat-transfer viscous flows, and turbulence-constrained problems [19, 20]; Yu et al. improved the stability and manufacturability of optimized channels using the moving morphable component method [21]. In recent years, topology optimization has also been applied to regenerative cooling channel design for hypersonic engines, and related studies have shown that it can improve flow distribution, heat-transfer efficiency, and wall-temperature uniformity [22–26]. Zhang et al. verified the heat-transfer advantage of topological channels over straight channels in non-uniform thermal environments [27], and Jing et al. demonstrated their potential to reduce pressure drop, suppress stagnation, and lower maximum temperature under complex local structural constraints [28]. Overall, existing studies have shown that topology optimization can overcome the limitations of regular channel design, but the flow and heat-transfer differences between topology-optimized channels and conventional straight channels under coupled fluid-volume, power-consumption, and complex thermal-boundary constraints still require further quantification.

Based on this background, this paper selects a typical structural component of a scramjet combustor as the research object and conducts fluid-thermal coupling topology optimization design for regenerative cooling channels. Given the heat source, coolant inlet conditions, and structural constraints, a topology optimization model is established to minimize the average temperature of the design domain while considering constraints on fluid volume fraction and power consumption. The cooling channel configuration is obtained on the OpenFOAM platform. A three-dimensional regenerative cooling structure is then constructed, and the topology-optimized channel is compared with a conventional straight channel in terms of flow resistance, flow distribution, wall temperature, and heat-transfer characteristics. The feasibility and advantages of topology optimization for lightweight and efficient thermal protection structure design are evaluated.

2. Problem Statement

Figure 1 shows a typical structural component of a scramjet combustor and the topology optimization computational domain. According to the geometric characteristics of the research object and the design requirements of the cooling channel, the combustor wall structure is extracted and reasonably simplified as the topology optimization design domain. Because the structure and boundary conditions are symmetric, only half of the full topology optimization region is used in the actual optimization to reduce computational cost and improve efficiency.

The design domain consists of a rectangular region with dimensions of 100 mm $\times$ 13.75 mm and six inlets/outlets with dimensions of 4 mm × 2 mm. The spacing between adjacent inlets/outlets is 2 mm. The inlets/outlets are 1 mm from the symmetry plane and 2.75 mm from the upper boundary. During computation, a uniform volumetric heat source of 1×10^8 W/m^3 is applied in the design domain. The coolant inlet velocity is set to 0.05 m/s, and the inlet temperature is 300 K.

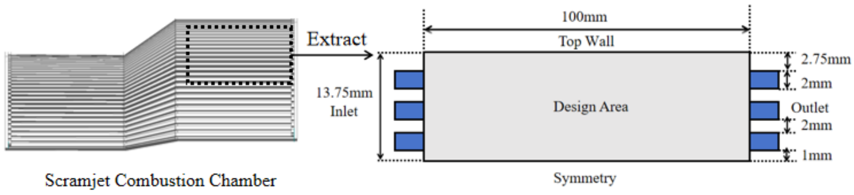

Figure 1: Topology optimization design domain.

3. Methods

3.1 Topology Optimization Model

This study adopts the density method to establish a fluid-thermal coupling topology optimization model. The design variable γ represents the local fluid-solid property, where $\gamma = 1$ denotes the fluid region and $\gamma = 0$ denotes the solid region. Material interpolation and a porous-medium penalization term are used to realize a continuous transition between the fluid and solid regions. The optimization objective is to minimize the average temperature of the design domain, while constraining the fluid volume fraction and power consumption to account for cooling capacity, pressure drop, and structural occupancy. In this study, the fluid volume constraint is set to 0.6.

The governing equations of the fluid-thermal coupling topology optimization model are

$$\nabla \cdot \mathbf{u} = 0, \tag{1}$$

$$\rho(\mathbf{u} \cdot \nabla)\mathbf{u} = -\nabla p + \mu \nabla^2 \mathbf{u} + \mathbf{F}, \tag{2}$$

$$\nabla \cdot (\rho \mathbf{u} C_p T) - \nabla \cdot [\lambda(\gamma)\nabla T] - Q = 0. \tag{3}$$

Here, $\mathbf{u}$ is the velocity vector, p is pressure, T is temperature, ρ is fluid density, μ is dynamic viscosity, C_p is the specific heat capacity, $\lambda(\gamma)$ is the effective thermal conductivity, and Q is the volumetric heat source. $\mathbf{F}$ is the body force introduced by the porous-medium penalization term to suppress flow in the solid region:

$$\mathbf{F} = -\alpha \mathbf{u}. \tag{4}$$

Here, α is the inverse permeability coefficient. It approaches zero in the fluid region and takes a large value in the solid region, thereby distinguishing the fluid channel from the solid material through velocity penalization. The RAMP interpolation between α and the design variable γ is used to ensure continuity and numerical stability:

$$\alpha(\gamma) = \alpha_{\max} \frac{q(1-\gamma)}{q+\gamma}. \tag{5}$$

The material thermal conductivity is also interpolated by the design variable γ to describe fluid heat transfer and solid conduction in a unified computational domain:

$$\lambda(\gamma) = \lambda_f + (\lambda_s - \lambda_f)\frac{\theta(1-\gamma)}{\theta+\gamma}. \tag{6}$$

The subscripts f and s denote the fluid and solid materials, respectively, and θ is an interpolation adjustment parameter.

The optimization model uses the average temperature of the design domain as the objective function and imposes constraints on power consumption and fluid volume fraction. The average temperature characterizes the overall thermal-protection performance, the power-consumption constraint limits pressure drop, and the volume constraint limits channel occupancy, thereby avoiding channels that are too narrow, excessively curved, or difficult to realize in engineering.

$$\begin{aligned}&\text{Find } \gamma,\\ &\text{Minimize } \Psi,\\ &\text{s.t.} \quad J < J_1, \qquad \frac{1}{|\Omega|}\int_\Omega \gamma \, d\Omega < V.\end{aligned} \tag{7}$$

The objective function and power-consumption constraint are

$$\Psi = \frac{1}{|\Omega|}\int_\Omega T \, d\Omega, \tag{8}$$

$$J = -\int_{\Gamma_{\text{in}}\cup\Gamma_{\text{out}}} \left(p + \frac{1}{2}\mathbf{u}\cdot\mathbf{u}\right)(\mathbf{u}\cdot\mathbf{n})\, d\Gamma. \tag{9}$$

GH3218 and n-decane are used as the solid material and fluid coolant, respectively. Considering the variable properties of n-decane at high temperature and high pressure, a two-dimensional temperature-pressure property table is established with CoolProp without considering cracking reactions, and local properties are obtained by linear interpolation in the computation. The table intervals are 3 K in temperature and 1 kPa in pressure. Compared with direct CoolProp calculations, the maximum error occurs near the supercritical region at approximately 650 K and is less than 0.1%, satisfying the requirements of numerical simulation.

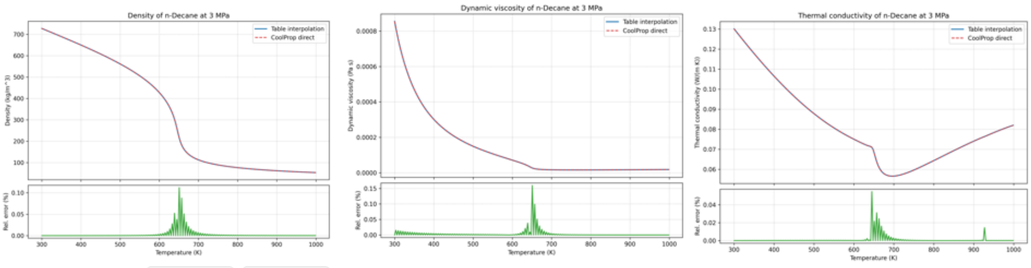

Figure 2: Thermophysical properties at 3 MPa.

To improve numerical stability and suppress checkerboard patterns and gray elements, Helmholtz filtering and Heaviside projection are applied sequentially to the design variables during optimization. Filtering reduces mesh-scale effects, and projection promotes convergence toward clear fluid-solid boundaries:

$$-r^2\nabla^2\bar{\gamma} + \bar{\gamma} = \gamma. \tag{10}$$

Here, r is the filter radius and $\bar{\gamma}$ is the filtered design variable. The Heaviside projection method is then used to further remove gray elements and obtain a more distinct geometric boundary:

$$\tilde{\gamma}_e = \frac{\tanh(\beta\eta) + \tanh[\beta(\bar{\gamma}_e - \eta)]}{\tanh(\beta\eta) + \tanh[\beta(1-\eta)]}. \tag{11}$$

Based on the above model, a fluid-thermal coupling topology optimization solver is constructed on the OpenFOAM platform. The solution procedure includes primal-variable solution, adjoint-variable solution, objective and constraint calculation, sensitivity filtering and projection, and MMA design-variable update. Both the primal and adjoint equations are solved iteratively using the SIMPLE algorithm.

The fluid thermophysical properties are updated through table interpolation, and the final cooling channel distribution satisfies the volume, power-consumption, and heat-source conditions.

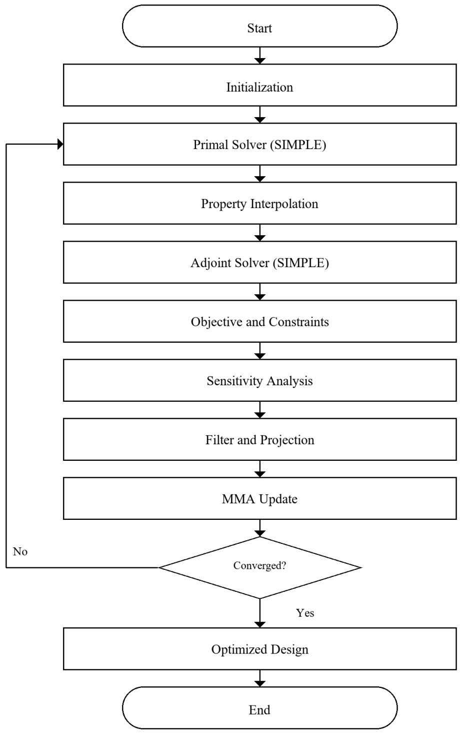

Figure 3: Solver workflow.

The final optimization result is shown in Figure 4. Driven by the average-temperature minimization objective, the cooling channel adaptively adjusts the fluid path according to the heat-source distribution and flow-resistance constraint in the design domain, forming a connected structure with branching characteristics between the inlet and outlet. Compared with a conventional regular channel, the topology-optimized channel enhances cooling capacity in high-heat-load regions under a limited fluid volume fraction, improves the overall temperature uniformity of the design domain, and provides a basis for subsequent three-dimensional numerical simulations and comparisons of flow and heat-transfer performance.

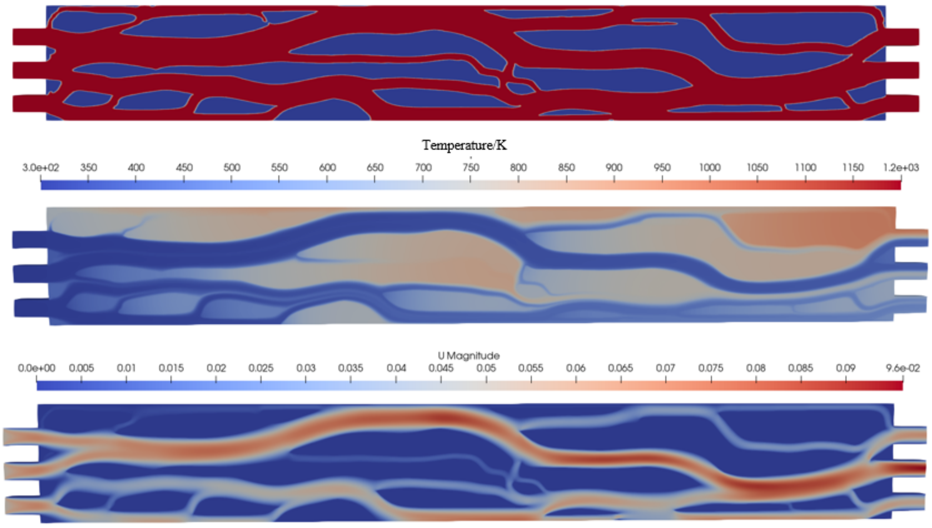

Figure 4: Topology optimization result.

3.2 Three-Dimensional Flow and Heat Transfer Model

A three-dimensional regenerative cooling model is constructed from the topology optimization result. The combustor wall consists of the inner wall, channel layer, and outer wall. The inner and outer walls are made of GH3128 alloy, and each of the three layers has a thickness of 2 mm. The two-dimensional topology result is stretched in the spanwise direction to obtain the channel-layer structure, as shown in Figure 5. Three-dimensional numerical simulations of flow and heat transfer are then performed based on this model.

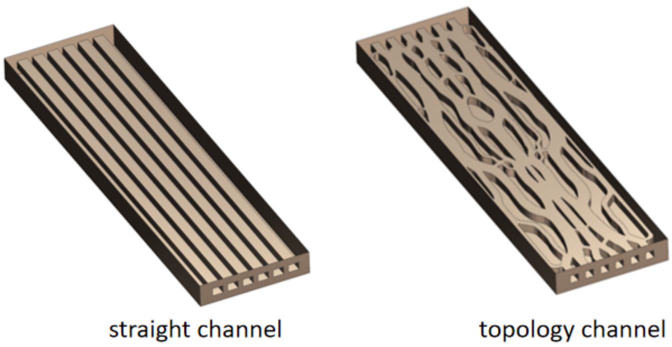

Figure 5: Three-dimensional model based on topology optimization.

In the Reynolds-averaged Navier–Stokes (RANS) calculations, the standard k-ε model is adopted for turbulence closure. Numerous numerical studies have shown that this model provides reliable predictions of flow and heat transfer for hydrocarbon fuels at supercritical pressure in horizontal channels. Pressure-velocity coupling is handled using a coupled algorithm, while the convective and diffusive terms are discretized using second-order upwind and second-order central-difference schemes, respectively.

HF-I endothermic hydrocarbon fuel developed by Tianjin University is used as the coolant [29]. HF-I is a mixture of multiple hydrocarbons, and the species and chemical pathways involved in endothermic cracking are highly complex. Therefore, a surrogate-species model is used in the simulations to represent the cracking reactions. In this study, a reduced three-step global reaction mechanism containing 17 species is adopted to simulate the endothermic cracking of kerosene under supercritical pressure. In this mechanism, $C_{11.85}H_{23.82}$ is used as the surrogate formula for kerosene, and the corresponding cracking mechanism is listed in Table 1. This endothermic model has been calibrated and assessed in previous work by the research group [27, 28]. The results show that the supercritical cracking model predicts fluid temperature with high accuracy and that the wall-temperature error is less than 5%.

Table 1: Three-step cracking mechanism for RP-3.

Reaction	A	Temperature exponent	E_a (J/mol)
$C_{11.85}H_{23.82} \rightarrow 0.1086H_2 + 0.4773CH_4 + 0.5586C_2H_4 + 0.39C_2H_6 + 0.41C_3H_6 + 0.2001C_3H_8 + 0.2246C_4H_8 + 0.0353C_4H_{10} + 0.031C_4H_6 + 0.4857C_5^+ + 0.5112CC_5^+ + 0.0222C_9H_{12}$	2.87×10^{14}	0	2.179×10^5
$C_5^+ \rightarrow 0.14H_2 + 0.48CH_4 + 0.39C_2H_4 + 0.45C_2H_6 + 0.055C_3H_6 + 0.355C_4H_8 + 0.0955C_4H_{10} + 0.0355C_4H_6 + 0.1091C_9H_{12}$	1.23×10^{12}	0	1.896×10^5
$CC_5^+ \rightarrow 0.7488C_6H_6 + 0.1396C_7H_8 + 0.05043C_8H_{10} + 0.03402C_8H_8 + 0.04262C_9H_{12}$	9.69×10^{12}	0	1.944×10^5

Based on the topology-optimized model described above, three-dimensional numerical simulations of regenerative-cooling flow and heat transfer are carried out. The inlet pressure, inlet mass flow rate, and heat flux imposed on the heated surface are set to 3 MPa, 0.0126 kg/s, and 2 MW/m^2, respectively. Simulations are performed for different fluid volume fractions and different inlet-temperature conditions, and the detailed operating conditions are listed in Table 2.

Table 2: Operating conditions.

Case	Channel configuration	Fluid volume fraction	T_{in} (K)	P_{in} (MPa)	$\dot{m}$ (kg/s)	q (MW/m^2)
1	Straight channel	0.42	300	3	0.0126	2
2	Topology-optimized channel	0.57	300	3	0.0126	2
3	Straight channel	0.57	300	3	0.0126	2
4	Straight channel	0.57	600	3	0.0126	2
5	Straight channel	0.57	800	3	0.0126	2
6	Topology-optimized channel	0.57	600	3	0.0126	2
7	Topology-optimized channel	0.57	800	3	0.0126	2

This study first compares the flow and heat-transfer capabilities of the topology-optimized and straight-channel structures under different fluid volume fractions. The results are shown in Table 3. In Case 2, the average heated-surface temperature is 1000 K and the maximum temperature is 1090 K, both significantly lower than those of the straight-channel configuration, indicating that the topology-optimized channel has stronger cooling capability for the hot wall. Compared with Case 1, Case 2 reduces the average and maximum heated-surface temperatures by 15.1% and 14.8%, respectively. Compared with Case 3, Case 2 reduces the average and maximum heated-surface temperatures by 17.5% and 16.5%, respectively. Meanwhile, the solid volume fraction of Case 2 is 26% lower than that of Case 1, showing that the topology-optimized channel reduces the channel-layer structural mass while lowering the average temperature.

Table 3: Performance comparison under different fluid volume fractions.

Case	T_{out} (K)	$\dot{m}_{out}$ (kg/s)	Cracking rate	Mean heated-surface T (K)	Maximum heated-surface T (K)	Δp (kPa)
1	411	0.0216	1.2%	1178	1280	0.50
2	422	0.0216	0	1000	1090	1.13
3	391	0.0216	5.6%	1212	1305	0.25

The temperature contours on the heated surface are shown in Figure 6. The results indicate that the straight-channel heated surface contains a more continuous high-temperature region, whereas the topology-optimized channel has a lower and more uniform temperature field overall. Figure 7 further shows that multiscale branches and connected networks form inside the topology-optimized channel. These networks redistribute the coolant from the mainstream direction toward near-wall regions, strengthening transverse transport and local convective heat transfer. The enhanced heat transfer of the topology-optimized configuration is accompanied by a certain flow-resistance penalty. The inlet-outlet pressure drop in Case 2 is 1.13 kPa, higher than the 0.50 kPa of Case 1 and the 0.25 kPa of Case 3. This shows that the complex branching structure increases local resistance losses while improving cooling performance.

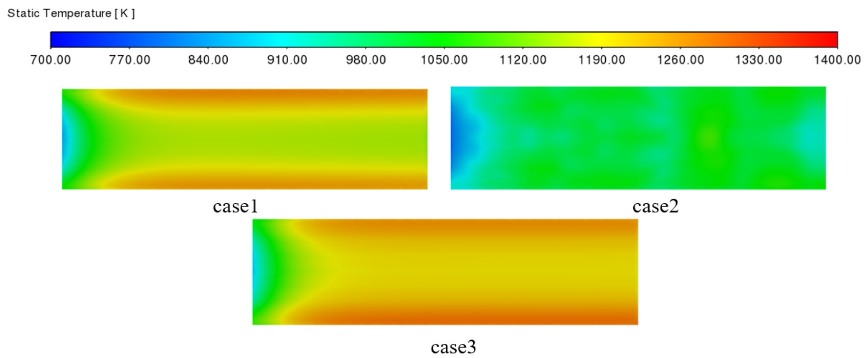

Figure 6: Temperature contours on the heated surface under different fluid volume fractions.

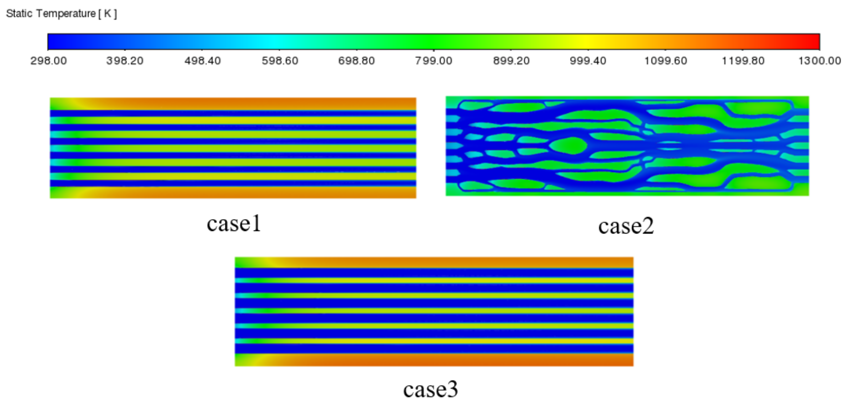

Figure 7: Temperature contours on channel cross-sections under different fluid volume fractions.

The flow and heat-transfer capabilities of the topology-optimized and straight-channel structures are then compared under different inlet temperatures at the same fluid volume fraction. Cases 2, 6, and 7 are topology-optimized configurations, whereas Cases 3, 4, and 5 are straight-channel configurations. The three comparisons correspond to low-, medium-, and high-temperature inlet conditions, respectively. Under the same fluid volume fraction, the topology-optimized configuration exhibits lower heated-surface temperatures than the corresponding straight channel for all three inlet-temperature conditions.

Under the low-temperature condition, the average and maximum heated-surface temperatures of Case 2 decrease by 17.5% and 16.5%, respectively, compared with Case 3. Under the medium-temperature condition, the average and maximum heated-surface temperatures of Case 6 decrease by 5.6% and 6.4%, respectively, compared with Case 4. Under the high-temperature condition, the average and maximum heated-surface temperatures of Case 7 decrease by 3.3% and 4.4%, respectively, compared with Case 5.

Table 4: Performance comparison under different inlet temperatures.

Case	T_{out} (K)	$\dot{m}_{out}$ (kg/s)	Cracking rate	Mean heated-surface T (K)	Maximum heated-surface T (K)	Δp (kPa)
4	666	0.0216	4.4%	1203	1287	0.82
5	844	0.0216	7.1%	1221	1307	4.35
6	673	0.0216	0.7%	1136	1205	1.89
7	852	0.0216	13%	1181	1249	7.2

These results show that, under the same volume fraction, the topology-optimized channel still lowers the hot-wall temperature, indicating that its cooling advantage mainly comes from channel-layout optimization rather than a simple increase in fluid volume fraction. In addition, as the temperature level increases, the relative cooling benefit of the topology-optimized channel over the straight channel gradually decreases. The enhanced cooling effect is most pronounced under the low-temperature condition.

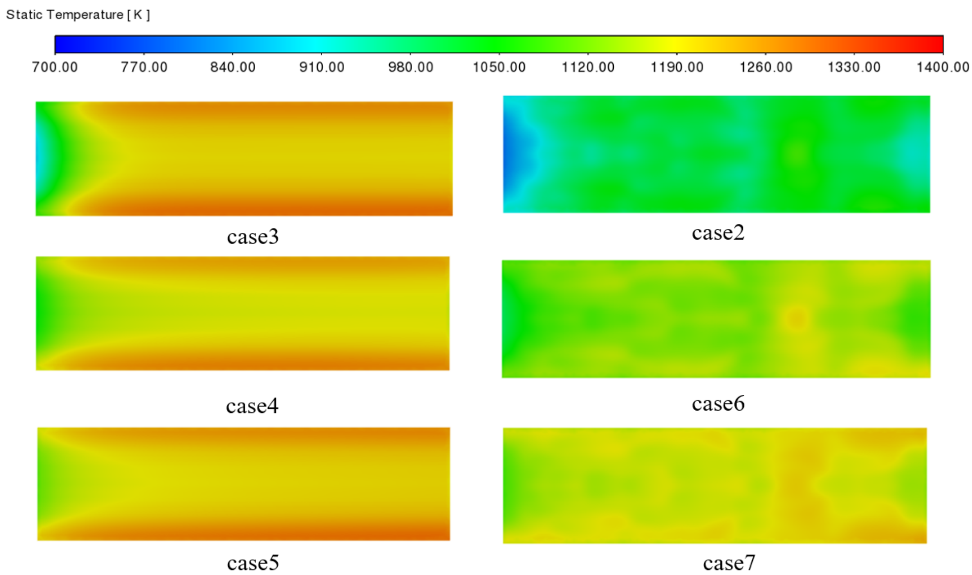

Figure 8: Temperature contours on the heated surface under different inlet temperatures.

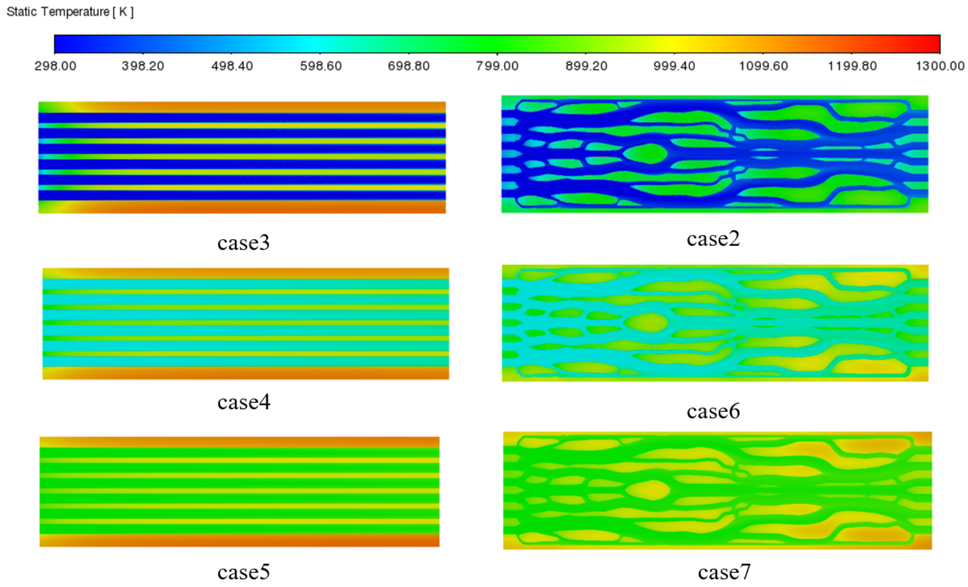

Figure 9: Temperature contours on channel cross-sections under different inlet temperatures.

4. Conclusion and Future Work

The design of regenerative cooling channels using topology optimization is expected to improve flow-distribution uniformity and heat-transfer efficiency, thereby enabling more efficient wall thermal protection. In this study, three-dimensional numerical simulations are used to evaluate the cooling performance of a topology-optimized cooling plate under RBCC engine heat-flux conditions. The main conclusions are as follows:

1. In terms of mass, the solid-domain fraction in the channel layer is 43% for the topology-optimized configuration and 58% for the straight-channel configuration, corresponding to a 26% mass reduction in the channel layer.

2. The topology-optimized channel in Case 2 has an average heated-surface temperature of 1000 K and a maximum temperature of 1090 K, both lower than those of the straight channels under different fluid volume fractions. This indicates that the topology-optimized configuration can effectively improve the wall-cooling capability of regenerative cooling channels.

3. Under the same volume fraction, the topology-optimized configuration still has a cooling advantage over the straight-channel configuration. The average and maximum temperatures are reduced by 17.5% and 16.5% under the low-temperature condition, by 5.6% and 6.4% under the medium-temperature condition, and by 3.3% and 4.4% under the high-temperature condition.

4. The cooling effect of the topology-optimized channel mainly originates from coolant redistribution by the branching network and enhanced transverse heat transfer. This advantage is most obvious under the low-temperature condition, and the relative temperature reduction decreases as the temperature level increases.

The results indicate that topology optimization is a feasible and effective computational design tool for regenerative cooling systems in scramjet engines. Future work will focus on additive manufacturing of topology-optimized regenerative cooling components and direct-connect ground thermal assessment tests of scramjet combustors, further promoting the engineering application of topology optimization in aerospace engines.

Acknowledgements

The authors appreciate the supports of the National Natural Science Foundation of China (Grant No. 52302478).

References

[1] Rui Xue, Xin He, Feixing Liu, Xiaogang Ma, Xing Zheng, Jianxun Du, and Chao Weng. A survey on the conceptual design of hypersonic aircraft powered by rbcc engine. *Proceedings of the Institution of Mechanical Engineers, Part C: Journal of Mechanical Engineering Science*, 237(18):4213–4245, 2023.

[2] L. Shi, G. J. Zhao, Y. Y. Yang, et al. Research progress on ejector mode of rocket-based combined-cycle engines. *Progress in Aerospace Sciences*, 107:30–62, 2019.

[3] Min Chen, Hailong Tang, Kun Zhang, Ouyang Hui, and Yanjun Wang. Turbine-based combined cycle propulsion system integration concept design. *Proceedings of the Institution of Mechanical Engineers, Part G: Journal of Aerospace Engineering*, 227(7):1068–1089, 2013.

[4] Fei Qin, Zheng Zhao, Guoqiang He, Tingting Jing, Xing Sun, and Xianggeng Wei. Thermal structure technology development of rocket based combined cycle engine. *Acta Aeronautica et Astronautica Sinica*, 45(11):529572, 2024.

[5] S. L. Zhang, X. Li, J. Y. Zuo, et al. Research progress on active thermal protection for hypersonic vehicles. *Progress in Aerospace Sciences*, 119:100646, 2020.

[6] Shibin Luo, Dequan Xu, Jian Liu, et al. A review of regenerative cooling technologies for scramjets. *Applied Thermal Engineering*, 190:116754, 2021.

[7] Ning Wang, Yu Pan, and Jin Zhou. Research status of active cooling of endothermic hydrocarbon fueled scramjet engine. *Proceedings of the Institution of Mechanical Engineers, Part G: Journal of Aerospace Engineering*, 227(11):1780–1794, 2013.

[8] Ni He, Chaoyang Liu, Yu Pan, and Jian Liu. Progress of coupled heat transfer mechanisms of regenerative cooling system in a scramjet. *Energies*, 16(3):1025, 2023.

[9] Tingting Jing, Guoqiang He, Fei Qin, et al. An innovative self-adaptive method for improving heat sink utilization efficiency of hydrocarbon fuel in regenerative thermal protection system of combined cycle engine. *Energy Conversion and Management*, 178:369–382, 2018.

[10] Shuhei Takahashi, Singo Demise, Mitsutosi Oshita, Takehisa Ikeda, Mitsuhiro Tsue, Kazunori Wakai, Yasushige Ujiie, and Michikata Kono. Relation between combustion mode and wall heat flux in a scramjet combustor. *Journal of the Japan Society for Aeronautical and Space Sciences*, 50(579):142–149, 2002.

[11] Qingchun Yang, Jichao Hu, Juntao Chang, Youhai Zong, and Wen Bao. Experimental study on combustion mode transition effects in a strut-based scramjet combustor. *Proceedings of the Institution of Mechanical Engineers, Part G: Journal of Aerospace Engineering*, 229(4):764–771, 2015.

[12] Renshuo Zhu, Xinyan Pei, Sihan Zou, et al. Flow distribution of supercritical hydrocarbon fuel in parallel regenerative cooling channels under non-uniform heat flux. *Propulsion and Energy*, 1:4, 2025.

[13] Jian Liu, Mengyao Xu, Kai Ma, Chaoyang Liu, and Wenxiong Xi. Heat transfer and flow structures of supercritical n-decane in a regenerative cooling channel loaded with non-uniform heat flux. *Frontiers in Energy Research*, 10:985220, 2022.

[14] T. Borrvall and J. Petersson. Topology optimization of fluids in stokes flow. *International Journal for Numerical Methods in Fluids*, 41(1):77–107, 2003.

[15] A. Gersborg-Hansen, O. Sigmund, and R. B. Haber. Topology optimization of channel flow problems. *Structural and Multidisciplinary Optimization*, 30(3):181–192, 2005.

[16] C. Othmer, E. de Villiers, and H. G. Weller. Implementation of a continuous adjoint for topology optimization of ducted flows. AIAA Paper 2007–3947, 2007.

[17] C. Othmer. A continuous adjoint formulation for the computation of topological and surface sensitivities of ducted flows. *International Journal for Numerical Methods in Fluids*, 58(8):861–877, 2008.

[18] U. Nilsson. Description of adjointshapeoptimizationfoam and how to implement new objective functions. In *Proceedings of CFD with OpenSource Software*, 2013.

[19] T. Matsumori, T. Kondoh, A. Kawamoto, and T. Nomura. Topology optimization for fluid-thermal interaction problems under constant input power. *Structural and Multidisciplinary Optimization*, 47:571–581, 2013.

[20] E. A. Kontoleontos, E. M. Papoutsis-Kiachagias, A. S. Zymaris, D. I. Papadimitriou, and K. C. Giannakoglou. Adjoint-based constrained topology optimization for viscous flows, including heat transfer. *Engineering Optimization*, 45(8):941–961, 2013.

[21] Minghao Yu, Shilun Ruan, Xinyu Wang, Zheng Li, and Changyu Shen. Topology optimization of thermal-fluid problem using the mmc-based approach. *Structural and Multidisciplinary Optimization*, 60(1):151–165, 2019.

[22] Xi Zhao, Mingdong Zhou, Ole Sigmund, and Casper S. Andreasen. A poor man's approach to topology optimization of cooling channels based on a darcy flow model. *International Journal of Heat and Mass Transfer*, 116:1108–1123, 2018.

[23] Joe Alexandersen, Niels Aage, Casper S. Andreasen, and Ole Sigmund. Topology optimisation of natural convection problems. *International Journal for Numerical Methods in Fluids*, 76(10):699–721, 2014.

[24] Janus Asmussen, Joe Alexandersen, Ole Sigmund, and Casper S. Andreasen. A poor man's approach to topology optimization of natural convection problems. *Structural and Multidisciplinary Optimization*, 59(4):1105–1124, 2019.

[25] M. Pietropaoli, F. Montomoli, and A. Gaymann. Three-dimensional fluid topology optimization for heat transfer. *Structural and Multidisciplinary Optimization*, 59:801–812, 2019.

[26] Joe Alexandersen and Casper S. Andreasen. A review of topology optimisation for fluid-based problems. *Fluids*, 5(1):29, 2020.

[27] Ting Zhang, Tingting Jing, Fei Qin, Xing Sun, Wenqiang Li, and Guoqiang He. Topology optimization of regenerative cooling channel in non-uniform thermal environment of hypersonic engine. *Applied Thermal Engineering*, 219:119384, 2023.

[28] Tingting Jing, Ting Zhang, Xing Sun, Fei Qin, Guoqiang He, and Ao Tian. Topology optimization design of regenerative cooling channels around the inserted pylon in hypersonic engine. *Applied Thermal Engineering*, 263:125282, 2025.

[29] Rongpei Jiang, Guozhu Liu, and Xiangwen Zhang. Thermal cracking of hydrocarbon aviation fuels in regenerative cooling microchannels. *Energy & Fuels*, 27:2563–2577, 2013.